Published by
NIGERIAN SOCIETY OF PHYSICAL SCIENCES
Available online @ https://journal.nsps.org.ng/index.php/jnsps

J. Nig. Soc. Phys. Sci. 5 (2023) 1609

Journal of the Nigerian Society of Physical Sciences

Synthesis and characterization of silica xerogel and aerogel from rice husk ash and pulverized beach sand via sol-gel route

K. M. Omatola[a,*], A. D. Onojah[b], A. N. Amah[b], I. Ahemen[b]

[a]*Department of Physics, Kogi State University, Anyigba, Nigeria*
[b]*Department of Physics, Joseph Sarwuan Tarka University of Makurdi, Benue State, Nigeria*

Abstract

The high cost and toxicity associated with the use of orthosilicates as silica precursors drive growing interest in an environmentally friendly and cost - efficient natural silica source. Rice husk (a biomass) and beach sand are both natural and non - toxic and the extraction of silica from each using sodium hydroxide makes the process green for the production of nanosilica gels (xerogel and aerogel) via the sol – gel route. The gels from the ash of rice husk and pulverized beach sand were dried by the use of a laboratory oven and supercritical extraction methods. The structures of the gels were studied through X-ray diffraction (XRD), transmission electron microscopy (TEM), selected area electron diffraction (SAED), scanning electron microscopy (SEM), X - ray fluorescence (XRF) spectroscopy and Fourier transform infrared (FTIR) spectroscopic analyses. XRF spectroscopy revealed silicon in its oxide form as the prominent element with low levels of trace elements concentrations. XRD results showed the crystalline nature of the prepared silica. TEM images confirmed the crystalline and nanometric structures of the streak - free xerogel and aerogel. SAED confirmed that the gels were polycrystalline with no streaks. SEM monographs showed varied globes of fine surfaces indicating the high level of purity of the gels. FTIR showed the absorption peaks of the silanol-OH bond and Si-O-Si vibration, confirming the gels as nanometric structures. The high yield, crystalline nature, purity and crystallographic features of the produced silica suggest rice husk ash and pulverized beach sand as alternative silica sources for the production of silica gels nanoparticles with potential applications in biomedical field, nanofiltration and as additive for improving the strength of materials.

DOI:10.46481/jnsps.2023.5.1609

Keywords: Rice husk ash, Pulverized beach sand, Sol-gel route, Drying techniques, Xerogel, Aerogel

Article History :
Received: 13 June 2023
Received in revised form: 12 August 2023
Accepted for publication: 23 October 2023
Published: 13 November 2023

Communicated by: E. A. Emile

1. Introduction

Nanosilica gels are among the lightest and most porous synthetic solid materials in existence and were synthesised first by Samuel Kistler [1]. They are rigid 3D network of colloidal structures, that exist as acqua-gel (hydrogel), alcolgel (gel with alcohol as a liquid medium) and depending on the drying technique, as xerogel- hydrogel or alcogel dried with oven and aerogel- hydrogel or alcogel dried with a supercritical extraction technique [2].

Silica gels were originally prepared from various sol-gel precursors like tetramethylorthosilicate (TMOS), tetraethylorthosilicate (TEOS) and polyethoxydisiloxane (PEDS), which are considered expensive and toxic in recent times [3]. Recent scientific efforts are geared towards sourcing for cheaper, safer

*Corresponding author: Tel.: +234-805-350-7607;
Email address: omatola@yahoo.com (K. M. Omatola)

and readily available natural silica precursors like rice husk and beach sand for the synthesis of nanosilica gels. Rice husk yields 20% ash made of 90 -98% silica [4],while sand consists of 60% silica [5], which makes both economical sources of sodium silicate as a precursor for the synthesis of nanosilica gels. It becomes imperative to look elsewhere for alternative sources of silica. Rice husks and beach sand are silica-based materials that can address the above shortcoming, as they are readily available in Nigeria.

Nowadays, the various nations of the world are diversifying their income generating sources through agriculture by going into more expansive rice production as well as naturally occurring materials. The husk from the rice can be a disposal problem; however, using it as a precursor for silica can avert the environmental problems associated with its disposal and open incineration.

Silica gels in nanometric dimensions have found applications in high-energy physics as detectors, in shock wave studies, inertial confinement, radio-luminescent and micrometeorites [2]. Other areas of applications include safety device manufacturing, adsorption, catalysts, carriers and fillers in composite materials [6].

There are numerous growing procedures for nanosilica gels, namely spray flame pyrolysis, sol-gel with ethanol solvent, ultrasonification with surfactant addition, sol - gel with calcinations, wet chemical method, dry method, hydrothermal/co-precipitation and alkali fusion route [7]. Each of these methods has one or more advantages over the others.

The sol – gel with ethanol solvent technique is adopted for this work because it requires low temperatures, is very economical, fast and simple and gives opportunity for the control of reaction kinetics via the variation of the composition of the reactants, which are vital in the growth of nanomaterials [8]. Furthermore, sol - gel technology is the best alternative for the growth of silica nanoparticles because of its ability to adjust the geometric outlook and particle size during a chemical process [9]. In addition, the sol-gel method is reported to offer high flexibility in the synthesis of a long range of photonic materials in a variety of configurations like monoliths, coatings, fibers and films for optical device utilization [9].

The techniques employed to dry hydrogel or alcogel can play a prominent role in influencing the structural and compositional parameters of the nanosilica gels and the performance of devices fabricated from the gels.

The present research work reports the green synthesis of silica gels from rice husk ash and pulverized beach sand via the sol – gel route, the drying of the gels with an oven and carbon dioxide supercritical methods and their characterizations. The produced nanosilica materials show properties that are consistent with silica prepared from toxic precursors such as TMOS, TEOS and PEDS.

2. Experimental Details

2.1. Synthesis of the gels

The sol-gel technique was employed to synthesize the nanosilica gels. The rice husk and beach sand were locally obtained from Idah local government area of Kogi state, Nigeria. Analytical - grade hydrochloric acid, sulphuric acid, sodium hydroxide, ethanol and n - hexane were used as reagents.

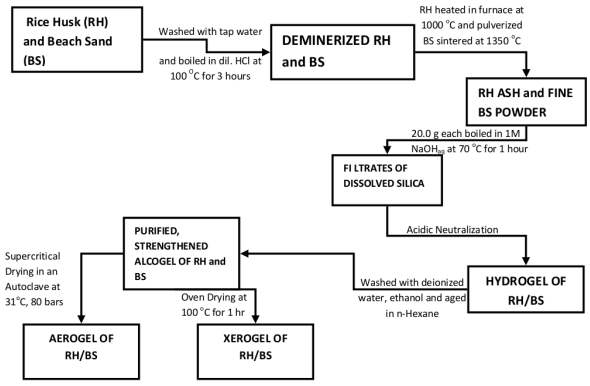

Figure 1. Experimental flowchart for the growth of the silica xerogel and aerogel.

The rice husk and beach sand were separately washed with tap water thereafter boiled in dilute hydrochloric acid for 3 hours at a temperature of 100 °C for demineralization. The demineralized samples were separately dried in an oven. The rice husk was converted to rice husk ash and following the technique reported by Sajid et al [10], a hydrogel was produced. However, the beach sand was pulverized and sintered at 1350 °C, thereafter sieved to obtain fine powdered adopting the methods reported by Nayak & Datta [11] and Munasir et al [12] a hydrogel was produced. The synthesis procedure is presented in Figure 1.

2.2. Assemblage of the supercritical dryer

Figure 2 represents the fabricated dryer used for the supercritical drying of the alcogels synthesized in this work. It consists of an autoclave (reacting chamber) as a vessel containing the n – hexane, the alcogels from rice husk and beach sand; a pressure gauge for monitoring of the pressure of the reacting chamber. Other parts include an inlet valve for the inflow of the liquefied CO_2, a safety valve, an exit or outlet valve where the supercritical fluid exits and a manifold as a connecting line between the reaction chamber and the CO_2 tank.

2.3. Characterization techniques

The Phillips PW-1210 type TEFA ORTEC automatic XRF machine was used with the following specifications: generator tension of 40KV, current of 25mA, CuKα1 (λ = 1.645 Å), CuKα2 (λ = 1.455 Å) and tube anode of Cu was used to evaluate the elemental composition of the gels by weight.

The XRD patterns of the dried nanosilica gels were obtained with the use of a Rigaku Miniflex Diffractometer of an EMPYREAN system with a CuKα radiation (λ = 1.5406 Å) with a step size of 0.026 and a continuous scan time of 23.97 s. The generator setting was at a voltage of 45 KV and a current of 40 mA, while the goniometer radius was set to 240 mm.

The crystallographic parameters of the gels were evaluated following the match of the XRD peak values with the major

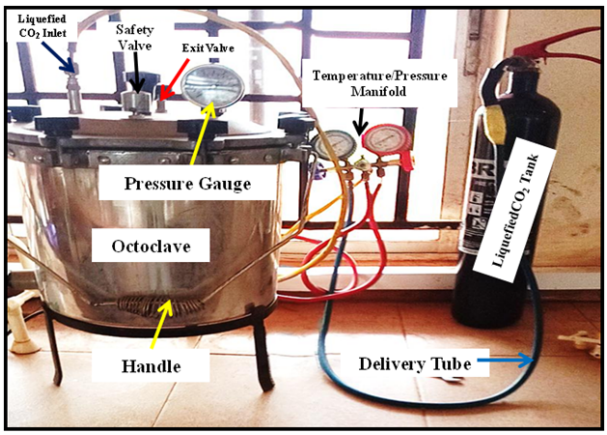

Figure 2. Assemblage of supercritical extraction equipment used.

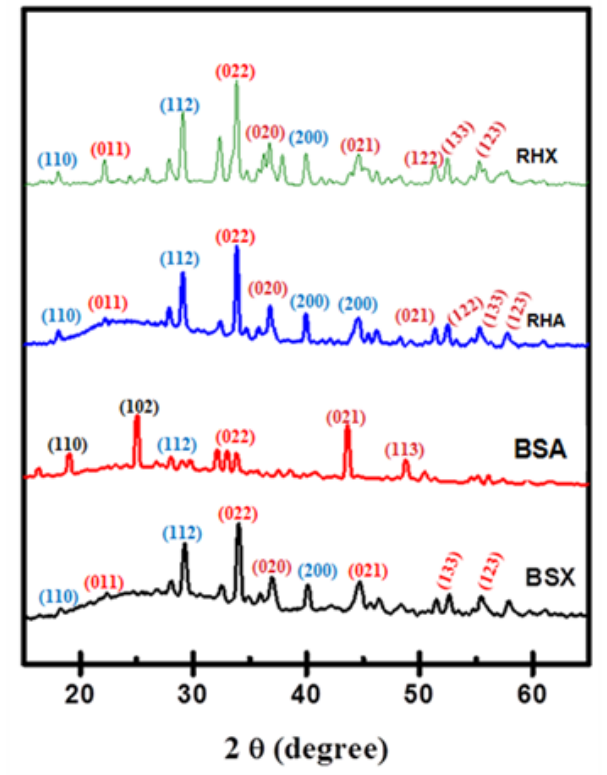

Figure 3. XRD spectra of the nanosilica xerogels and aerogels showing alignment and slight shifts in the reflection peaks.

elements (Si, Ca, K, Al and Na) as obtained from the x – ray fluorescence (XRF) spectroscopy analysis with the aid of the MATCH-3 software version of the crystallographic open database (COD) system for phase identification and indexing.

The morphology of the gels was investigated with the use of JEM-ARM200F-G transmission electron microscope (TEM). Selected area electron diffraction (SAED) was used to measure the crystallinity of the silica gels.

Fourier transform infrared (FTIR) spectroscopy was used to obtain the infrared spectra within a scan range of 4400 – 350 cm^{-1} wavelength in transmittance mode.

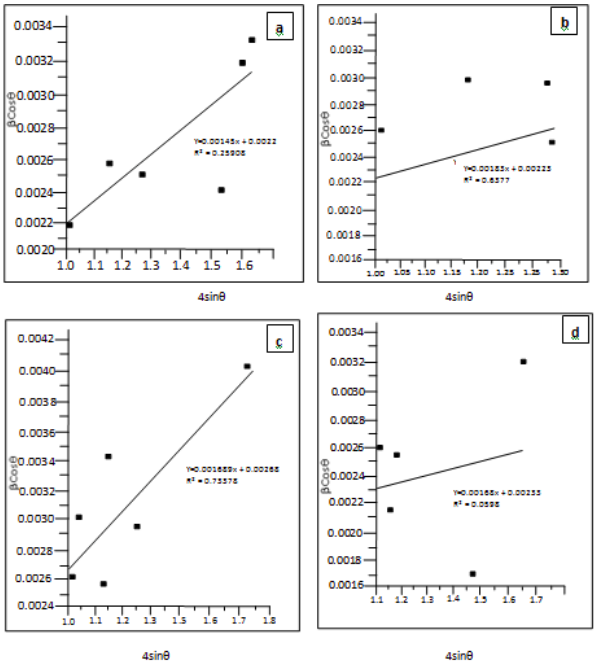

Figure 4. (a) W – H plot for RHX (b) W – H plot for RHA (c) W – H plot BSX (d) W – H plot for BSA.

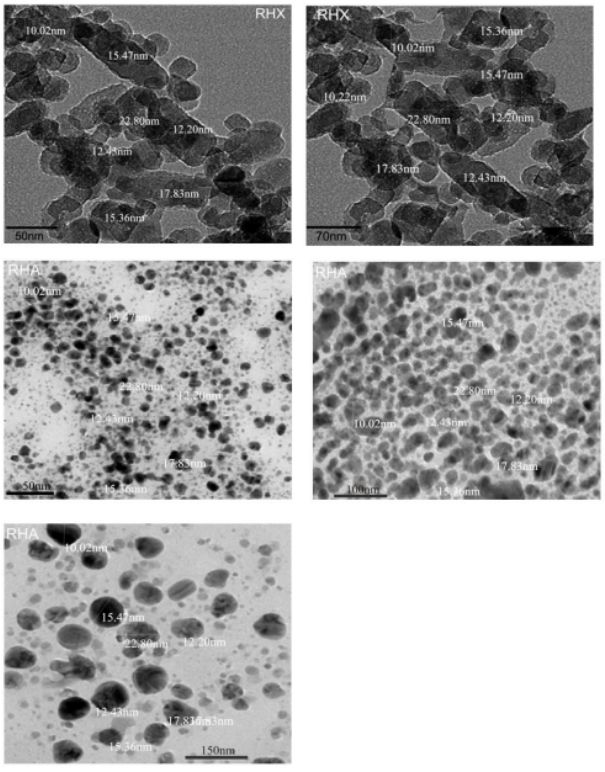

Figure 5. (a - b)TEM images of rice husk xerogel with average crystallite diameter of 14.9 nm (c - e) TEM images of rice husk aerogel with crystallite diameter of 14.7 nm.

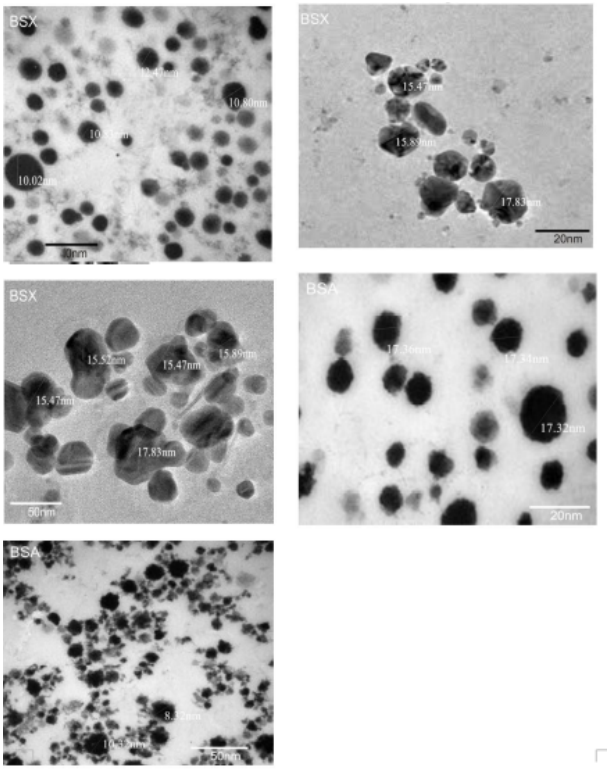

Figure 6. (a - c) TEM images of beach sand xerogel with average crystallite diameter of 14.5 nm and (d - e) TEM images of beach sand aerogel with average crystallite size of 13.3 nm.

3. Results and Discussion

3.1. Elemental composition of the xerogels and aerogels

Table 1 shows elemental composition of the produced silica materials. For the rice husk, the total impurity (trace elements) in the xerogel was 9 % by weight, resulting in a high level of purity of the gel, whose SiO_2 (silica) content weighs 75.50 %. On the other hand, the total impurity in the aerogel was 9.22% by weight, signifying a high level of purity of SiO_2 weighing 80.20 %. The highest impurity came from Ca, K and Al. The amount of SiO_2 in the aerogel was found to be higher as compared to the xerogel, indicating its higher yield. However, the percentage weight of silica in the beach sand xerogel and aerogel is 56 % and 57 %, respectively, with both showing a lesser level of purity when compared to the gels from the rice husk. Another remarkable observation is the complete absence of phosphoric oxide in both the gels from the beach sand source, which is likely because the sand is not obtained from a farmland where fertilizer could have been used to improve crop yield [13]. The rice husk - based gels have an associated oxide of minute phosphorus possibly taken up by the rice from the soil during paddy growth. The silica from the rice husk is greater in quantity and richer in quality, which suggests its preference over that from beach sand for mass production.

3.2. Crystallographic features of the xerogels and aerogels

Figure 3 shows the XRD patterns of the silica xerogels (RHX), (BSX) and aerogels (RHA), (BSA), synthesized from rice husk and beach sand, respectively. Several sharp diffraction peaks could be observed, revealing that the produced materials are crystalline in nature [14]. The RHA and BSX exhibit a broad hump around 2θ of 20 – 24°, which is an attribute of the amorphous phase of silicon [11, 15]. A weak, narrow diffraction peak (2θ) situated around the 22° could be seen on the hump. The existence of the broad peak but low hump, to-

Table 1. Percentage weight composition of the silica gels from XRF spectrophotometer.

Compounds/ Elements	Rice Husk (RH)		Beach Sand (BS)	
	Xerogel (RHX)	Aerogel (RHA)	Xerogel (BSX)	Aerogel (BSA)
SiO_2	75.5	80.2	56.39	56.57
Al_2O_3	2.2	2	24.6	24.42
Fe_2O_3	0.15	0.15	4.66	4.59
TiO_2	0.2	0.2	1.13	1.2
CaO	2.25	2.75	1.66	1.65
P_2O_5	0.02	0.02	-	-
K_2O	3.42	3.45	0.89	0.9
MnO	0.04	0.41	0.07	0.06
MgO	0.01	0.01	3.69	3.7
Na_2O	0.12	0.14	6.87	6.85
Ba	0.0863	0.0856	0.099	0.1141
Cu	0.0021	0.0019	0.0023	0.0158
Cr	0.0048	0.0013	0.0022	0.0177
Ni	0.001	0.0016	0.0022	0.0083
Zn	0.004	0.0013	0.001	0.012
Co	0.0011	0.001	0.0012	0.0046
Sr	0.0042	0.0005	0.001	0.0189
Pb	0.002	0.0012	0.002	0.0011
Sc	0.0008	0.001	0.003	0.009
Cd	1E-05	2E-05	2E-05	0.0011

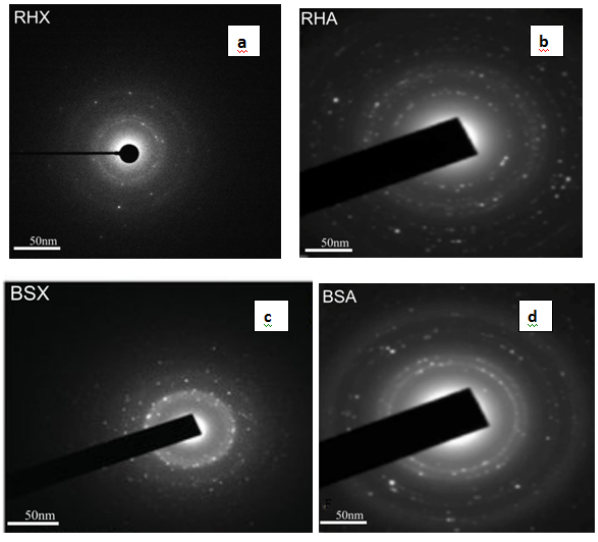

Figure 7. (a) SAED pattern of rice husk xerogel (b)SAED pattern of rice husk aerogel (c) SAED pattern of beach sand xerogel and (d) SAED pattern of beach sand aerogel.

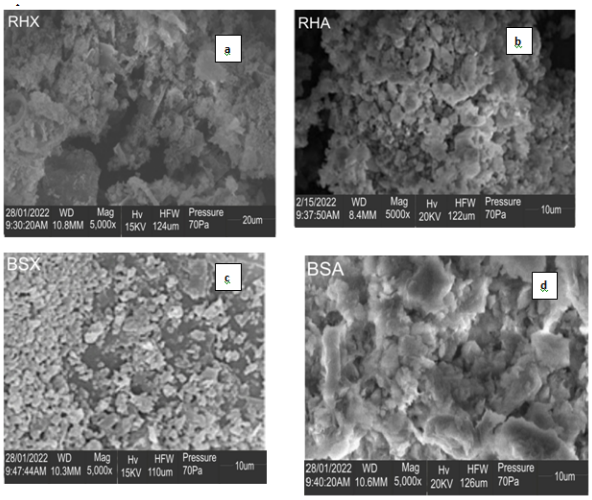

Figure 8. SEM monographs at 5000x magnification (a) scanned monograph of rice husk xerogel (b) scanned monograph of rice husk aerogel (c) scanned monograph of beach sand xerogel (d) scanned monograph of beach sand aerogel.

gether with the sharp peak at 22° in the rice husk gels, suggests the crystalline nature of the produced silica. The XRD patterns of the RHX and BSA do not exhibit a hump, which indicates the relatively high crystalline nature of the grown gels. Additional sharp diffraction peaks could be observed for all the XRD patterns, indicating the presence of ordered crystalline structures [4]. The crystalline silica described in this work is consistent with the report by Ref. [10] but inconsistent with the several previous studies that confirmed that silica synthesized from rice husk ash has an amorphous structure and seldomly exhibits additional crystallite diffraction peaks [11, 16–19]. The inconsistency is attributable to the calcination temperature of the raw rice husk at 1000 °C and pulverized beach sand to 1350 °C, which agrees with the assertion that amorphous silica transforms to crystalline phase if fired to 1000 °C and beyond [20]. There is an alignment in the most intense reflection peaks (2θ) at 34° for the RHX, RHA and BSX but a slight shift (misalignment) in the positions of the peaks for the BSA. This misalignment or shift in peaks suggests that a structural change occurs in the beach sand gels during the drying process [21].

The average crystallite size was estimated using two methods, Refs. [22, 23], the Derby – Scherer method (Eq. 1) and Williamson – Hall method (Eq. (2)). The Scherer method is the most simplified formulation for crystallite analysis [10, 14] and shows that the peak width is inversely proportional to crystallite size. On the other hand, W – H method assume that the diffraction line broadening is traceable not only to crystallite size but also to strain contribution and varies quite differently with respect to Bragg angle [24].

$$D = k\lambda/\beta\cos\theta, \tag{1}$$

$$\beta_{hkl}\cos\theta = \left(\frac{k\lambda}{D_{W-H}}\right) + 4\varepsilon_{W-H}\sin\theta, \tag{2}$$

where D is the Scherer size or average crystallite size, λ = 0.15406 nm is the wavelength of the x- ray source for Cu, β is the full width at half maximum (FWHM) in radians, θ is the Bragg's angle, k is a shape factor numerically equal to 0.9. However, D_{W-H} is the Williamson – Hall size or crystallite size that could be determined from the Williamson – Hall plot (Figure 4(a - d)), ε_{W-H} is the microstrain that could be obtained from the slopes of the graphs and β_{W-H} is the full width at half maximum for W – H plot. According to the W – H method, the average size of the crystallites could be estimated by substituting the y – intercept into Eq. (2).

The crystallite size estimated from the Scherer method was found to be 60 nm and 61 nm for the xerogel and aerogel, respectively, for the rice husk. On the other hand, the W – H method yielded 62 nm and 63 nm for the xerogel and aerogel, respectively. However, the crystallite size obtained from the Scherer method was found to be 51 nm and 63 nm for the xerogel and aerogel, respectively, for the beach sand. On the other hand, the W – H method yielded the size 52 nm and 59 nm for the xerogel and aerogel, respectively. Both methods confirm that RHA and BSA exhibit relatively large crystallite sizes. The difference in the crystallite size obtained using Scherer method and W – H method could be attributed to the strain contribution to the W – H size [21].

Based on the crystallite sizes obtained, it is reasonable to classify the grown xerogel and aerogel materials into soft and hard silica, respectively. A larger size implies hard nanosilica gel and vice versa [24]. Therefore, the aerogel is structurally tougher and harder than the xerogel.

The dislocation density is a measure of irregularity in a crystal due to growth accident or drying process. It can be calculated from Eq. (3) [25]. The dislocation density denotes the number of dislocation lines per unit volume of crystal. In other words, the dislocation density value illustrates the degree of crystallinity of the xerogel and aerogel nanoparticles profiles

$$\delta = \frac{1}{D^2}. \tag{3}$$

The dislocation density was calculated using the crystallite derived from the W – H method, because the method is reported to be more accurate [21]. The dislocation density of the rice husk xerogel was found to be 2.6×10^{-2} lines per nm^2, while that of the rice husk aerogel was 2.5×10^{-2} lines per nm^2. The value of the dislocation density for the beach sand xerogel was found to be 3.7×10^{-2} lines/nm^2, while the aerogel was 2.8×10^{-2} lines /nm^2. The relatively small values for the RHA and BSA suggest that the aerogel material has less disorder compared to xerogel (RHX and BSX). This slight decline in the dislocation density implies that gels dried using the supercritical method (under controlled temperature and pressure) show less disorder compared to gels dried via the oven (under only temperature controlled condition). Meanwhile, the calculated values of dislocation density for the RHX and BSX indicate a high degree of crystallinity, as seen in the sharp peaks of the XRD results.

The lattice strain is a measure of the distribution of lattice parameters arising from crystal defects like dislocation and grain boundaries [26] and it increases with increasing crystallite size [27]. The W – H strain from (Figure 4(a – d)) was found to

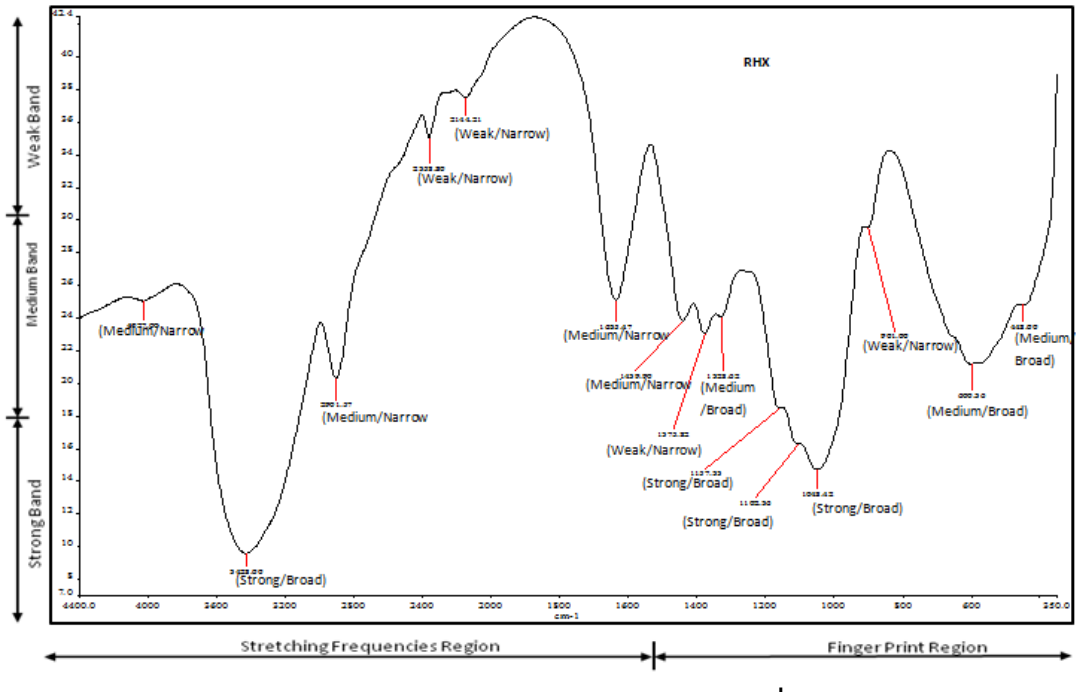

Figure 9. FTIR spectrum of rice husk silica xerogel.

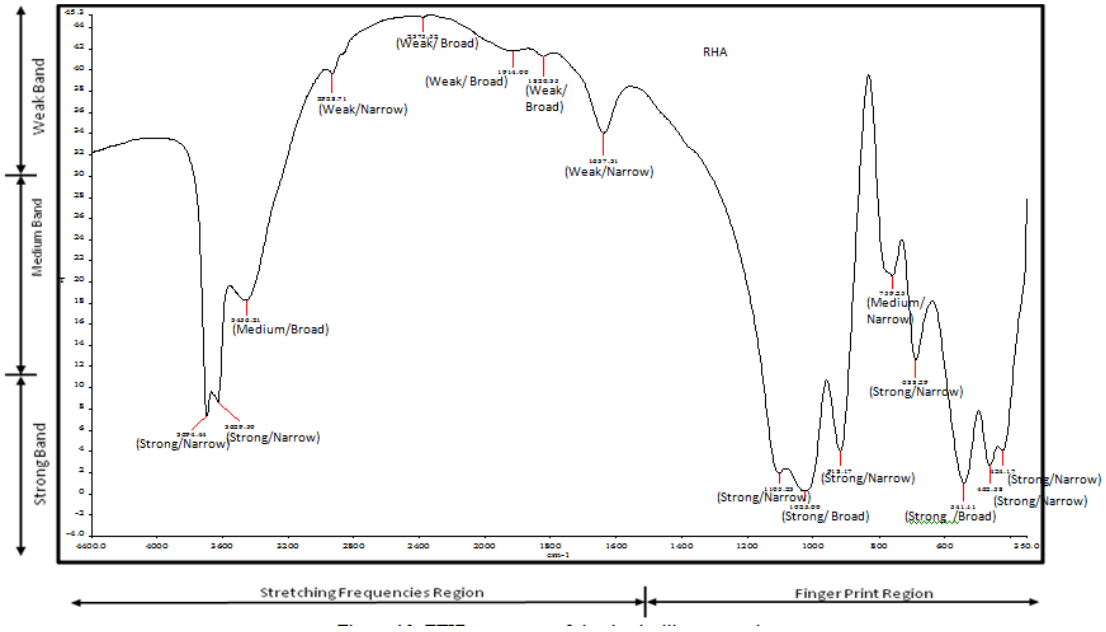

Figure 10. FTIR spectrum of rice husk silica aerogel.

be 1.8×10^{-3} and 1.5×10^{-3} for the rice husk xerogel and aerogel, respectively. These strain values are consistent with the values obtained according to Ref. [10]. Meanwhile the strain obtained for the beach sand xerogel and aerogel, respectively, is 1.7×10^{-3} and 1.1×10^{-3}.

3.3. TEM images of the silica gels

Figure 5 shows the TEM results obtained for the xerogel and aerogel of the rice husk ash. (Figure 5 (a -b)) shows that the crystallites of the xerogel have an elongated shape with varied diameters and an average size of 14.9 nm. The TEM image of the aerogel (Figure 5 (c - e)) revealed dispersed spherical shape of crystallites with average diameter of 14.7 nm.

Figure 6 (a -c) showed dispersed oval shapes with an average crystallite diameter of 14.5 nm for the beach sand xerogel and Figure 6 (d -e) revealed a mixture of rod –like and spherical shapes with an average crystallite diameter of 13.3 nm.

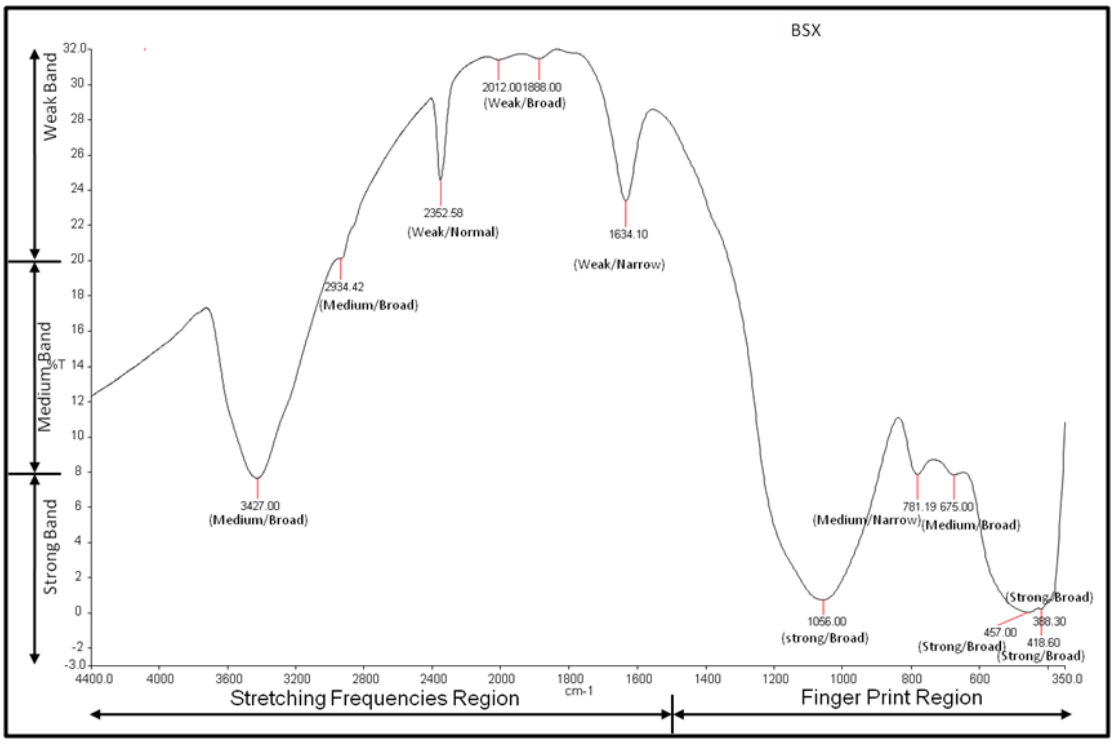

Figure 11. FTIR spectrum of beach sand silica xerogel.

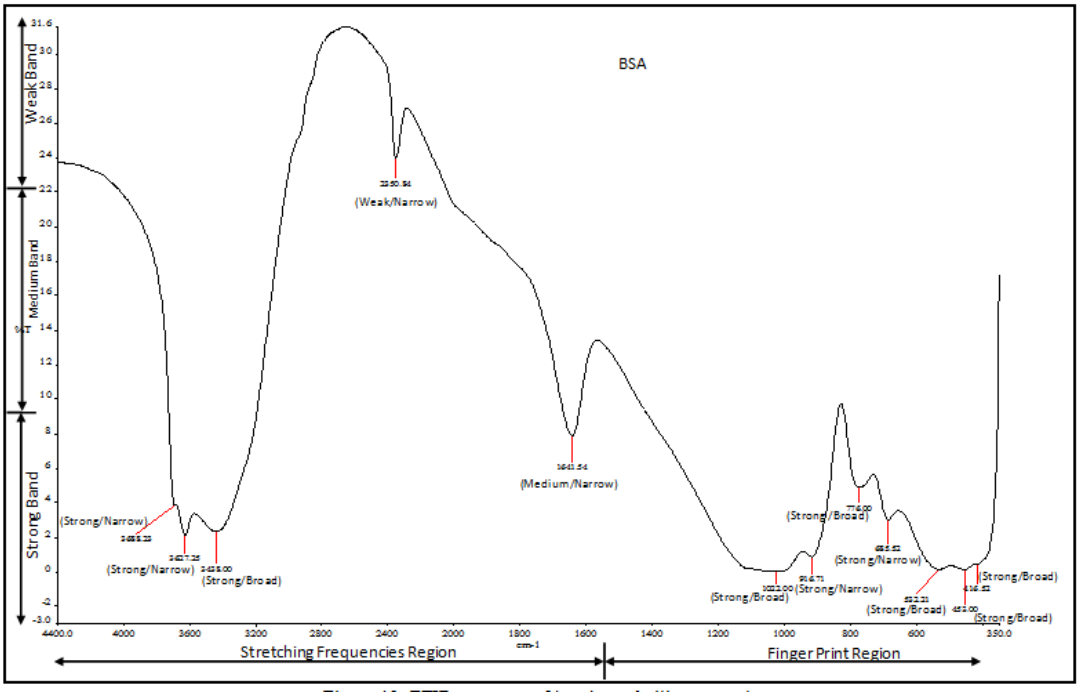

Figure 12. FTIR spectrum of beach sand silica aerogel.

The dimensions of the crystallite diameters in nanometric range showed that the particles of the gels are ultrafine [4], while the dissimilarity between the crystallite domain sizes and diameters of all the gels showed that the gels are polycrystalline [28].

3.4. *SAED patterns of the nanosilica gels*

Figure 7 represents the SAED patterns of the xerogel and aerogel of the rice husk and beach sand.The patterns for the xerogel and aerogel revealed bright spots and rings, confirming their crystalline nature, while the randomly dotted spots in ring forms confirmed that the gels are polycrystalline [28].

3.5. Density and Surface area of the silica gels

The calculated density of the rice husk xerogel was 3.31 g/cm^3 and that of aerogel was 2.86 g/cm^3, while those of the beach sand xerogel and aerogel were 2.88 g/cm^3 and 2.68 g/cm^3, respectively, using the crystallographic open data (COD). The variation in the density was due to the different drying techniques employed.The aerogel is lighter than the xerogel because the supercritical extraction method aided the replacement of the liquid component of the alcogel by air. The xerogel still contain some amount of liquid components.

Equation (4) [29] defines the specific surface area (SSA) in m^2/g:

$$SSA = 6/\rho dm, \tag{4}$$

where ρ represents density in g/cm^3 and d_m is the crystallite diameter in nanometers. The substitution of the respective values of the density and crystallite diameters of the xerogel and aerogel yielded the specific surface area values of 122 m^2/g and 145 m^2/g for the xerogel and aerogel, respectively, for the rice husk, which shows an increment of 16 %. However, the result of the substitution for the xerogel and aerogel of the beach sand shows 144 m^2/g and 168 m^2/g, representing an increment of 17%. The obtained SSA for the aerogel is found to be greater than that of the xerogel owing to the shrinkage associated with the xerogel not being dried under supercritical means [30]. These results affirmed the assertion that xerogels are associated with higher shrinkage or reduced volume, hence high density and lower specific surface area compared to aerogels of the same material [30]. Gels derived from the pulverized beach sand show enhanced surface area than those from rice husk ash, which suggests that they can be preferable to be used as liquid (stains and poisons) adsorbents and catalyst supports media or carriers [4] but aerogel is more preferable due to its higher surface area [31].

3.6. SEM monographs

Figure 8 represents the SEM monographs of the gels of both the rice husk and beach sand. The physical structures show the outer appearance of the gels derived from the rice husk ash and pulverized beach sand.

The SEM monographs showed varied globes of fine surfaces for both gels without hair like feature indicating the high level of purity associated the synthesized gels [7].

3.7. Fourier transform analysis

Figures 9 - 12 represent the FTIR spectroscopy of the xerogel and aerogel of the rice husk and beach sand, respectively. The spectra give the details of the major spectra regions and types of infrared bond vibrations that caused absorption in transmittance mode.

The peaks of the FTIR spectra in Figures 9 – 12 occurring between 3700 and 3200 cm^{-1} correspond to Si-OH compounds due to the reaction of silica with sodium hydroxide [1]. Peaks between 2400 and 2200 cm^{-1} are due to stretching vibration. Peaks from 980 to 800 cm^{-1} showed the formation of a Si-Cl bond due to the reaction of silica with HCl. Peak 1000 – 1100 cm^{-1} is characteristic of the Si – O bond in Si - O - Si while 1600 – 1650 cm^{-1} is characteristic of the double bond between Si – O due to the lone pair of electrons in the vacant d-orbital of the silicon atom. The peak at 1635.47 cm^{-1} can be assigned to Si-H_2O flexion [32]. It is generally observed that almost all the bonds lie within the finger print region of wavelength axes for silica gels.

4. Conclusion

Silica gels in the xerogel and aerogel regimes were produced from rice husk ash and pulverized beach sand via the sol – gel technique. XRF, XRD, TEM, SAED, SEM and FTIR analyses were used to study the prepared material. The XRF analysis revealed silicon oxide as the major component with little percentage impurity, although the rice husk produced a higher quantity and purer nanosilica. XRD results showed crystalline silica with an approximate crystallite size between 51 – 64 nm. TEM results revealed the polycrystalline structure of the gels without streaks. SEM supported the purity of the gels as the structures were smooth without hair – like features. The aerogel showed a relatively large surface area compared to the xerogel. FTIR indicated various absorption peaks that are consistent with a nanocrystalline material. The xerogel and aerogel produced from the rice husk ash and pulverized beach sand demonstrate properties that are comparable to those obtained from toxic orthosilicates. This reveals that rice husk and beach sand that are both natural in origin and non – toxic exhibit relatively high purity silica content are potential green sources for the extraction of nanosilica gels and therefore are promising low cost materials to replace the toxic and expensive synthetic orthosilicates.

References

[1] J. P. Nayak & J. Bera, "A simple method for production of humidity indicating silica gel from rice husk ash", Journal of Metals, Materials and Minerals **19** (2009) 15. https://doi.org/10.1080/0371750x.2009.11082163

[2] P. Ram & P. Monika, "Rice hush ash as a renewable source for the production of value added silica gel and its application: An overview", Bulletin Chemical Reaction Engineering and Catalysis **7** (2012) 1. https://doi.org/10.97671/BCREC.7.1.1216.1-25

[3] N. Meftah, A. Hani & A. Merdas, "Extraction and physiochemical characterization of highly – pure amorphous silica nanoparticles from locally available dunes sand", Chemistry Africa (2023) 1. https://doi.org/10.1007/s42250-023-00688-2

[4] J.N. Saleh, A. A. Abdulrahman & Z. A.Yousif, "Characterization of nano silica prepared from Iraqi rice husk and its application in oil well's cement", Journal of Petroleum Research and Studies **7** (2017) 236. https://doi.org/10.52716/jprs.v7i1.179

[5] D. Pallavi, B. Jatin & P. Dilip, "Determination of silica activity index and XRD, SEM and EDS", Indian Institute of Metals **65** (2012) 63. https://doi.org/10.1007/s12666-011-007-z

[6] V. H. Lee, C. H. Thuc & H. H. Thuc, "Synthesis of silica nanoparticles from Vietnamese rice husk by sol - gel method", Nano Research Letters **8** (2013) 58. https://doi.org/10.1186/1556-276X-8-58

[7] A. N. Azzahra, E. S. Yusefin, G. Salima, M. W. M. Mudita, N. A. Febriani & A. B. D. Nandiyanto, "Review: Synthesis of nanosilica materials from various sources using various methods", Journal of Applied Science and Environmental Studies **3** (2020) 254. https://doi.org/10.48393/IMIST.PRSM/jases-v3i4.23427

[8] R. S. Dubey, Y. B. R. D. Rajesh & M. A. More, "Synthesis and characterization of SiO_2 nanoparticles via sol – gel method for industrial applications, 4th International Conference on materials processing and characterization", Materials Today Proceedings **2** (2015) 3575. https://doi.org/10.1016/j.matpr.2015.07.098

[9] S. Rovani, J. J. Santos, P. Corio, D. A. Fungaro & J. Braz, "An alternative and simple method for the preparation of Bare silica nanoparticles using sugarcane waste ash: An abundant and despised residue in Brazilian industry", Journal of Chemical Society **30** (2019) 1524. https://doi.org/10.1021/acsomega.8b00092

[10] H. Sajid, K. S. Rakesh, S. K. Nishant & K. Gaurav, "Synthesis and characterization of crystalline nano silica from rice husk (agricultural waste) and its magnetic composites", Research Square (2022) 1. https://doi.org/10-21203/rs.3.rs-1785138/v1

[11] P. P. Nayak & A. K. Datta, "Synthesis of SiO_2 - nanoparticles from rice husk ash and its comparison with commercial amorphous silica through material characterization", Silicon Springer Nature **13** (2020) 1209. https://doi.org/10-1007/s12633-020-00509-y

[12] Z. Munasir, T. Tariwikantoro, Z. Mochamad & D. Darminto, "Synthesis of SiO_2 nanoparticles containing quartz and cristobalite phases from silica sands", Materials Science – Poland **33** (2015) 47. https://doi.org/10.1515/msp-2015-0008

[13] F. Mnthambala, E. Tilley, S. Tyrrel & R. Sakrabani, "Phosphorus flow analysis for Malawi: identifying potential sources of renewable phosphorus recovery", Resources, Conservation and Recycling **173** (2021) 105744. https://doi.org/10.1016/j.reconrec.2021.105744

[14] S. S. Oluyamo, O. F. Famutimi, & M. O. Olasoji, "Isolation and characterisation of high grade nanosilicon from coastal landform in Ilaje local government area of Ondo State, Nigeria", African Scientific Reports **2** (2023) 82. https://doi.org/10.46481/asr.2023.2.1.82

[15] K. E. Motlagh, N. Asasian-Kolur, & S. Sharifian, "A comparative study on rice husk and rice straw as bioresources for production of carbonaceous adsorbent and silica", Biomass Conversion and Biorefinery **12** (2022) 5729. https://doi.org/10-1007/s13399=020-01145-7

[16] R. A. Ar, M. Rizka, M. A. Alfie, D. A. Resa, R. Cut, A. Thamer, R. Ali, & U. A. S. Faiz, "Experimental study of the mechanical properties and microstructure of geopolymer paste containing nano-silica from agricultural waste and crystalline admixtures", Case Studies in Construction Materials **16** (2022) 14. https://doi.org/10-1016/j.cscm.2022.e00792

[17] D. Dorairaj, N. Govender, S. Zakaria & R. Wickneswari, "Green synthesis and characterization of UKMRC – 8 rice husk - derived mesoporous silica nanoparticle for agricultural application", Scientific Reports **12** (2022) 1. https://doi.org/10-1038/s41589-022-24484-z

[18] A. Jyoti, R. K. Singh, N. Kumar, A. K. Aman & M. Kar, "Synthesis and properties of amorphous nanosilica from rice husk and its composites", Materials Science and Engineering B **263** (2021) 14871. https://doi.org/10-1016/j.mseb.2020.114871

[19] I. J. Fernandes, D. Calheiro, F. A. L. Sanchez, A. L. D. Camacho, T. L. A. C. Rocha, C. A. M. Moraes & V. C. Sousa, "Characterization of silica produced from rice husk ash: comparison of purification and processing methods", Materials Research **20** (2017) 512. https://doi.org/10-1590/1980-5373-MR-2016-1043

[20] M. A. Azmi, N. A. A. Ismail, M. Rizamarhaiza, W. M. Hasif & H. Taib, "Characterization of silica derived from rice husk (Muar, Johor, Malaysia) decomposition at different temperatures", AIP Conference Proceedings **1756** (2016) 1. https://doi.org/10-1063/1.4958748

[21] P. R. Jubu, F. K. Yam & K. M. Chahrour, "Vacuum, Structural and morphological properties of β-Ga_2O_3 nanostructures synthesized at various deposition temperatures", Physica E **123** (2020) 1. https://doi.org/10-1016/j.physe.2020.114153

[22] E. A. Okoronkwo, P. E. Imoisili, S. A. Olubayode & S. O. O. Olusunle, " Development of silica nanoparticles from corncob ash", Advances in Nanoparticles **5** (2016) 135. https://doi.org/10-4236/anp.2016.52015

[23] P. R. Jubu, B. Yusuf, A. Abdulkadir, O. S. Obaseki, K. M. Chahrour, Y. Yusof, H. D. Dehiin, N. S. Akiiga, G. F. Newton, M. Umar, B. T. Terngu, U. F. Onah & A. J. Atsor, "Enhanced photoelectrochemical transient photoresponse properties of molybdenum oxide film deposited on black silicon", Materials Science & Engineering B **289** (2023) 1. https://doi.org/10-1016/j.mseb.2023.116260

[24] C. Torres, A. Lopez-Suarez, B. Can-Uc, R. Rangel-Rojo, L. Tamayo-Rivera & L. Oliver, "Collective optical Kerr effect exhibited by an integrated configuration of Silicon quantum dots and gold nano particles embedded in ion-implanted silica", Nanotechnology **26** (2015) 29571. https://doi.org/10-1088/0957-4484/26/29/295701

[25] I. W. Sutapa, A. W. Wahab. P. Taba & N. L. Nafie, "Dislocation, crystallite size distribution and lattice Strain of Magnesium Oxide nanoparticles", Journal of Physics Conference Series **979** (2018) 1. https://doi.org/10-1088/1742-6596/979/1/012021

[26] S. Sarka, S. D. Ramarao, T. Das, R. Das, C. P. Vinod, S. Chakraborty & S. C. Peter, "Unveiling the roles of lattice strain and descriptor species on Pt - like oxygen reduction activity in Pd-Bi catalysts", American Chemical Society Publications **11** (2021) 800. https://doi.org/10-1021/acscatal.Oc03415

[27] D. Kumar, M. Singh & A.K. Singh, "Crystallite size effect on lattice strain and crystal structure of $B_{1/4}Sr_{3/4}MnO_3$ layered perovskite manganite", American Institute of Physics **1958** (2018) 1. https://doi.org/10-1063/1.5032520

[28] C. F. Holder & R. E. Schaak, "Tutorial on Powder X- ray diffraction for characterizing nanoscale materials", American Chemical Society Nano **13** (2019) 7359. https://doi.org/10-1021/acsnano.9b05157

[29] N. Permatasari, T. N. Sucahya & A. B. S. Nandiyanto, "Review: Agricultural wastes as a source of silica material", Indonesian Journal of Science and Technology **1** (2016) 1. https://doi.org/10-17509/ijost.v1i1.2216

[30] A. K. Koopmann, T. Bartschmid & N. Husing, "Renewable organic and related carbon aerogel monoliths from polycondensation of Tannin 5-(Hydroxymethyl) furfural", Journal of Sol – Gel Science and Technology (2023) 1. https://doi.org/10-1007/s10971-022-06015-4

[31] K. Zik, L. Wang, Y. Zhang, Y. Jiang, L. Zhang & A. Yasin, "Influence of size and shape of silica supports on the sol – gel surface molecularly imprinted polymers for selective adsorption of gossypol", Materials **11** (2018) 777. https://doi.org/10-3390/ma1105077

[32] H. El- Rassy & A. C. Pierre, "NMR and IR spectroscopy of silica aerogels with different hydrophobic characteristics", Journal of non-crystalline solids **351** (2005) 1063. https://doi.org/10-1016/j.jnoncrysol.2005.03.048